JOURNAL OF AIRCRAFT
Vol. 45, No. 1, January–February 2008

Efficient Reliability-Based Design and Inspection of Stiffened Panels Against Fatigue

Amit A. Kale,* Raphael T. Haftka,† and Bhavani V. Sankar‡
University of Florida, Gainesville, Florida 32611

DOI: 10.2514/1.22057

This paper develops an efficient computational technique to perform reliability-based optimization of structural design and an inspection schedule for fatigue crack growth. Calculating structural reliability in the presence of inspection is computationally challenging because crack size distribution has to be updated after each inspection to simulate replacement. An exact evaluation using Monte Carlo simulation is time consuming because large sample size is required for estimating accurately a low probability of failure. In this paper a less expensive approximate method is proposed to calculate reliability with inspection, combining Monte Carlo simulation and a first-order reliability method. We use Monte Carlo simulation with a small sample to update the probability distribution of crack sizes after inspection and a first-order reliability method to calculate the failure probability at any time between inspections. The application of this methodology is demonstrated by optimizing structural design and an inspection schedule for minimum life cycle cost of stiffened panels subject to uncertainty in material properties and loading. The effect of the structural design and the inspection schedule on the operational cost and reliability is explored and the cost of structural weight is traded against inspection cost to minimize total cost. Optimization revealed that the use of inspections can be very cost effective for maintaining structural safety.

Nomenclature

A_s	=	area of a stiffener, m^2
A_{Total}	=	total cross sectional area of panel, m^2
a	=	crack size, mm
a_c	=	critical crack size, mm
a_{cH}	=	critical crack length due to hoop stress, mm
a_{cL}	=	critical crack length for transverse stress, mm
a_{cY}	=	critical crack length causing yield of net section of panel, mm
a_h	=	crack size at which probability of detection is 50%, mm
a_i	=	initial crack size, mm
$a_{i,0}$	=	crack size due to fabrication defects, mm
a_N	=	crack size after N cycles of fatigue loading, mm
b	=	panel length, m
C_{tot}	=	total cost, dollars
cov	=	coefficient of variation (standard deviation divided by mean)
D	=	Paris model parameter, $\text{m}^{1-\frac{\text{m}}{2}}(\text{MPa})^{-\text{m}}$
d	=	fastener diameter, mm
F_c	=	fuel cost per pound per flight, dollars
$F^{\max}_{\text{FirstStiffener}}$	=	maximum stress on first stiffener, MPa
$F^{\max}_{\text{SecondStiffener}}$	=	maximum stress on second stiffener, MPa
$F^{\max}_{\text{ThirdStiffener}}$	=	maximum stress on third stiffener, MPa
g	=	limit state function used to determine structural failure
h	=	panel width, m
I_c	=	inspection cost, dollars
K	=	stress intensity factor, MPa $\sqrt{\text{m}}$
K_{IC}	=	fracture toughness, MPa $\sqrt{\text{m}}$
l	=	fuselage length, m
M_c	=	material manufacturing cost per pound for aluminum, dollars
m	=	Paris model exponent, Eq. (1)
N	=	no. of cycles of fatigue loading
N_f	=	fatigue life, flights (flights, time, and cycles are used interchangeably in this paper)
N_i	=	no. of inspections
N_p	=	no. of panels
N_s	=	no. of stiffeners
N_{ub}	=	no. of intact stiffeners
Pf_{th}	=	threshold probability of failure, reliability constraint
P_d	=	probability of detection
P_f	=	failure probability
P_d^{rand}	=	random number for probability of detection
p	=	fuselage pressure differential, MPa
r	=	fuselage radius, m
S_l	=	service life (40,000 flights)
S_n	=	nth inspection time in number of cycles or flights
s	=	fastener spacing, mm
t	=	panel thickness, mm
t_s	=	stiffener thickness, mm
W	=	structural weight, lb
Y	=	yield stress, MPa
β	=	inspection parameter, Eq. (11)
β_d	=	reliability index
ρ	=	density of aluminum, lb/ft^3
σ	=	hoop stress, Mpa
ϕ	=	cumulative distribution function of standard normal distribution
ψ	=	geometric factor due to stiffening

Received 26 December 2005; revision received 31 December 2006; accepted for publication 2 January 2007.

*Graduate Student, Department of Mechanical and Aerospace Engineering. Student Member AIAA.
†Distinguished Professor, Department of Mechanical and Aerospace Engineering. Fellow AIAA.
‡Newton C. Ebaugh Professor, Department of Mechanical and Aerospace Engineering. Associate Fellow AIAA

I. Introduction

COMPUTATION of life expectancy of structural components is an essential element of aircraft structural design. The structural integrity of a component is affected by damage such as fatigue cracks in metal structures, accidental impact, and environmental factors like corrosion. The life of a structure cannot be accurately determined even in carefully controlled conditions because of variability in material properties, manufacturing defects, and environmental

factors. Because of this uncertainty, the damage tolerance approach to structural integrity has become popular in aerospace applications. Here we assume that damage in the form of cracks is present in the structure at all times and these cracks will be detected by inspection before they grow to a critical length during the operational life. Inspections are scheduled at fixed time intervals to detect fatigue cracks and also protect against unexpected accidental damage. The Federal Aviation Administration (FAA) requires that all structures designed for damage tolerance be demonstrated to avoid failure due to fatigue, manufacturing defects, and accidental damage (FAR 25.571 damage tolerance and fatigue evaluation of civil and transport category airplanes).

Reliability-based optimization is computationally expensive when inspections are involved because crack size distribution has to be recharacterized after each inspection to simulate replacement. Inspections improve the structural safety through damage detection and replacement. However, inspections cannot detect all damage with absolute certainty due to equipment limitations and human errors. Probabilistic models of inspection effectiveness can be used to incorporate the uncertainty associated with damage detection. Typically, the crack size distribution after an inspection will not have a simple analytical form and can only be determined numerically. Exact evaluation of failure probability following an inspection can be done by Monte Carlo simulation (MCS) with a large population which is computationally expensive. The high computational cost for estimating very low probabilities of failure combined with the need for repeated analysis for optimization of structural design and inspection times makes MCS cost prohibitive.

Harkness [1,2] developed a computational methodology to calculate structural reliability with inspections without updating the crack size distribution after each inspection. He assumed that repaired components will never fail again and incorporated this assumption by modifying the first-order reliability method (FORM). This expedites reliability computations which require only the initial crack size distribution to be specified. In previous papers [3,4], we used the same methodology to optimize the inspection schedule.

When inspections are needed earlier than half the service life, repaired components may have a large probability of failure. In this case Harkness's method may not be accurate enough. In this paper we propose an approximate method to simulate inspection and repair using MCS and estimate the failure probability using the FORM. MCS is computationally very expensive for evaluating low failure probabilities due to a large population requirement, but is cheap for estimating probability distribution parameters (e.g., mean and standard deviation). We use the data obtained from MCS to obtain the mean and standard deviation of crack size distribution. Subsequently, FORM was used to calculate the failure probabilities between inspections. The combined MCS and FORM approach to calculate failure probability with inspection removes the computational burden associated with using MCS alone.

This method was applied to combined optimization of the structural design and inspection schedule of fuselage stiffened panels. Stiffened panels are popular in aerospace applications. Stiffeners improve the load carrying capacity of structures subjected to fatigue by providing an alternate load path so that the load gets redistributed to stiffeners as cracks progress. Typical stiffening members include stringers in the longitudinal directions and frames, fail-safe straps and doublers in the circumferential direction of the fuselage. Fracture analysis of stiffened panels has been performed by Swift [5] and Yu [6]. They used displacement compatibility to obtain the stress intensity factor due to stiffening. Swift [5] studied the effect of the stiffener area, skin thickness, and stiffener spacing on the stress intensity factor. He also discussed failure due to fastener unzipping and the effect of stiffening on residual strength of the panel. Yu [6] also compared the results with finite element simulation.

It is easier to perform reliability-based structural optimization of safe-life structures than of fail-safe structures because the optimization of the former involves only structural sizes while for the latter the inspection regime also needs to be optimized. Nees and Canfield [7] and Arietta and Striz [8,9] performed safe-life structural optimization of F-16 wing panels to obtain the minimum structural weight for fatigue crack growth under a service load spectrum. For an aircraft fail-safe design, a reliability-based design has been applied to the design of the inspection schedules. Provan and Farhangdoost [10] used Markov chains to estimate failure probability of a system of components, and Brot [11] demonstrated that using multiple inspection types could minimize cost.

Fujimoto et al. [12], Toyoda-Makino [13], Enright and Frangopol [14], Wu et al. [15], Garbatov and Soares [16], and Wu and Shin [17] developed optimum inspection schedules for a given structural design to maintain a specified probability of failure. Wu and Shin [18] developed a methodology to improve the accuracy of reliability calculations with inspections.

In our previous paper Kale et al. [3] demonstrated the combined structural design and optimization of an inspection schedule of an unstiffened panel. The main objective of the present paper is to develop a cost effective computational methodology that allows one to perform reliability-based optimization of structural design and inspection schedule. The methodology is demonstrated by performing structural optimization and inspection scheduling of stiffened structures against fatigue. To reduce the computational time associated with fatigue life calculation and reliability analysis, response surface approximations are developed for tracking crack growth.

Section II outlines the damage growth model in a structure subjected to cyclic pressure loading. This section also discusses the structural design of fuselage panels and a probabilistic model for inspection effectiveness. Section III describes the computational method to perform reliability-based design optimization with an inspection schedule. Section IV shows results for combined optimization of a structural design and an inspection schedule, and Sec. V presents concluding remarks.

II. Crack Growth and Inspection Model

A. Fatigue Crack Growth

The rate of fatigue crack propagation can be expressed as a function of the applied stress intensity factor, crack size, and material constants (which are obtained by fitting the empirical model to the experimental data). For the example in this paper we use the Paris law:

$$\frac{\mathrm{d}a}{\mathrm{d}N} = D(\Delta K)^m \tag{1}$$

where $\mathrm{d}a/\mathrm{d}N$ is the crack growth rate in m/cycles, the stress intensity factor range ΔK is in MPa$\sqrt{\mathrm{m}}$, and m is obtained by fitting the crack growth model to empirical data. More complex models account for load history effects. The stress intensity factor range for a cracked stiffened panel can be calculated using the finite element or the analytical method as a function of stress σ and crack length a.

$$\Delta K = \psi\sigma\sqrt{\pi a} \tag{2}$$

The effect of stiffening on the stress intensity is characterized by the geometric factor ψ which is the ratio of the stress intensity factor for the cracked body to that of the stress intensity factor at the crack tip of an infinite plate with a through-the-thickness center crack. The calculation of ψ usually requires detailed finite element analysis. Here, ψ is calculated using a method due to Swift [5] briefly described in Appendix D. The number of fatigue cycles accumulated in growing a crack from the initial size a_i to the final size a_N can be obtained by integrating Eq. (1) between the initial crack a_i and final crack a_N. Alternatively, the final crack size a_N after N fatigue cycles can be determined from Eq. (3). This requires repeated calculation of ψ as the crack propagates.

$$N = \int_{a_i}^{a_N} \frac{\mathrm{d}a}{D(\Delta K)^m} \tag{3}$$

Here we focus on designing a fuselage panel for fatigue failure caused by hoop stresses. The hoop stress is given by Eq. (4) and the crack grows perpendicular to the direction of hoop stress (see Fig. 1).

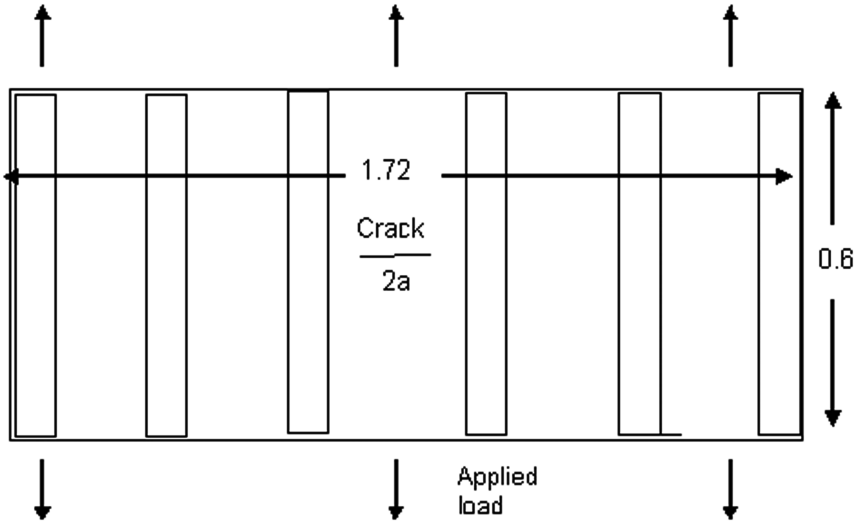

Fig. 1 Fuselage stiffened panel geometry and applied loading in hoop direction (crack grows perpendicular to the direction of hoop stress).

$$\sigma = \frac{rph}{th + N_s A_s} \tag{4}$$

B. Critical Crack Size

We consider optimizing the design of a typical fuselage panel for fatigue failure due to hoop stress. The fail-safe stiffening members in the circumferential direction such as frames, fail-safe straps, and doublers are modeled as equispaced rectangular rods discretely attached to the panel by fasteners. The panel size is assumed to be small compared to the fuselage radius so it was modeled as a flat panel following Swift [5]. We assume that only three stiffeners adjacent to the crack centerline are effective in reducing the stress intensity factor. So we model the aircraft fuselage structure by a periodic array of through-the-thickness center cracks with three stiffeners on either sides of the centerline as shown in Fig. 1. The critical crack length a_c at which failure will occur is dictated by considerations of residual strength or crack stability. Structural failure occurs if the crack size at that time is greater than the critical crack. The crack length causing net section failure is given by

$$a_{cY} = 0.5\left(h - \left[\frac{rph}{Yt} - \frac{N_{\text{ub}} A_s}{t}\right]\right) \tag{5}$$

Equation (5) gives the crack length a_{cY} at which the stress in the panel will exceed Y:

$$a_{cH} = \left(\frac{K_{IC}}{\psi\sigma\sqrt{\pi}}\right)^2 \tag{6}$$

$$a_{cL} = \left(\frac{K_{IC}}{\frac{pr}{2t}\sqrt{\pi}}\right)^2 \tag{7}$$

Equation (6) determines the critical crack length in fracture for failure due to σ and Eq. (7) determines the critical crack length for failure due to transverse stress. This is required to prevent fatigue failure in the longitudinal direction where skin is the only load carrying member (the effect of stringers in the longitudinal direction was not considered because hoop stress is more critical for fatigue). The critical crack length for preventing structural failure is given by Eq. (8)

$$a_c = \min(a_{cY}, a_{cH}, a_{cL}) \tag{8}$$

and N_f of the structure is determined by integrating Eq. (3) between a_i and a_c. Typical material properties for 7075-T651 aluminum alloy most commonly used in aerospace applications are as follows: yield stress $Y = 500.0$ MPa, crack size due to fabrication defect $a_{i,0}$ is lognormal (mean $= 0.0002$ m and standard deviation$=$ 0.00007 m), paris model exponent m is lognormal (mean $= 2.97$, standard deviation $= 1.05$), pressure load, p is lognormal (mean $= 0.06$, cov $= 5\%$) Mpa, fracture toughness $K_{IC}=$ 36.58 Mpa $\sqrt{\text{m}}$. The applied load due to fuselage pressurization is assumed to be 0.06 MPa (maximum pressure differential, 8.85 psi, Niu [19]). The Joint Service Specification Guide 2006 [20] specifies design assuming a minimum initial crack of 0.127 mm to exist in the structure at all times. However we consider a more conservative value of initial crack distribution (mean of 0.2 mm) to account for uncertainties associated with damage initiation and growth associated with corrosion, environmental effects, and accidental damage. The structural design parameters obtained for the B747 series aircraft from Niu [19] and *Jane's All the World's Aircraft* [21] are listed in Table 1.

C. Probability of Failure at a Given Time

The calculation of fatigue life of a structural component is based on the equivalent initial flaw method [20]. In addition, we assume that a threshold probability of failure is specified for a single panel. System failure can be calculated if data are available on the correlation coefficients between individual panels, but this is not considered here. Similarly, panel failure may occur due to extreme loads rather than fatigue, and this is not addressed in the present work because of its emphasis on computational improvements for design for fatigue.

Failure after N cycles of loading is defined as the event that fatigue life (number of cycles accumulated in growing a crack from the initial crack to a critical crack) is less that N. The purpose of reliability analysis is to determine the probability that the structure will not fail for a random realization of uncertain variables (a_i, m, and σ). The equation which defines the failure boundary is known as the limit state function, g. So for our case

$$g(a_i, m, \sigma) = N_f(a_i, m, \sigma) - N \tag{9}$$

Table 1 Structural design for fuselage [5,19,21]

Fastener diameter, d	4.8 mm
Fastener spacing, s	3.1 cm
Fuselage length, l	68.3 m
Fuselage radius, r	3.25 m
No. of panels, N_p	1350
No. of fasteners per stiffener	10
No. of stiffeners, N_s	6
Panel length, b	0.6 m
Panel width, h	1.72 m
Stiffener thickness, t_s	5 mm

where N_f is determined by integrating Eq. (3) between a_i and a_c. The failure probability corresponding to Eq. (9) is approximated using FORM. In this method the limit state function is represented in the transformed standard normal variables (a_i, m, and σ are transformed to normal distributions with mean = 0 and standard deviation = 1) and the point on the limit surface closest to origin is determined. This point is known as the most probable point and the shortest distance is called β_d. The calculation of the reliability index is an optimization problem solved by the MATLAB© [22] fmincon function (which employs sequential quadratic programming). The main reason for using FORM is that it is computationally cheaper than MCS. The failure probability is determined from the reliability index using the cumulative distribution function of the standard normal distribution.

$$P_f = \Phi(-\beta_d) \tag{10}$$

FORM provides only an approximation to the failure probability, whose accuracy needs to be checked for any given application. Appendix B compares the results using FORM to results obtained with 50×10^6 MCS samples to show very good agreement.

For an unstiffened panel, an analytical expression of fatigue life is available; however, for stiffened panels determining fatigue life requires a computationally expensive calculation of the geometric factor.

D. Inspection Model

When the structure is subjected to periodic inspections, cracks are detected and repaired or the structural part is replaced. We assume that the probability P_d, of detecting a crack of length a, is given by Palmberg's equation [23]:

$$P_d(a) = \frac{(a/a_h)^\beta}{1 + (a/a_h)^\beta} \tag{11}$$

An approximate value of a_h of 1 mm was obtained by rounding off data from the probability of detection curves in [24] for eddy current inspection. They obtained the probability of detection curves by machining artificial cracks in panels and counting the number of times they were detected after inspecting several times. The value of 3 of the other inspection parameter β was obtained by fitting Eq. (11) to the inspection data in that reference and increasing it slightly (to account for improvement in inspection technology since 1997). It is assumed that once a crack is detected, the panel is replaced by a newly manufactured panel with the fabrication defect distribution. This is not reasonable when we can detect very small cracks, and the present procedure allows us to consider a scenario where only cracks above a certain size trigger replacement of the panel. We have investigated this option in Appendix C and found that avoiding replacements for cracks under 0.9 mm has negligible effect on the probability of failure. For simplicity, the results presented here assume replacement for any detected crack, immaterial of size. However, inspection costs, which are based on an estimate of current practices are likely to reflect leaving very small cracks alone.

III. Computational Method to Perform Reliability-Based Optimization with Inspections

When inspection and replacement of structural components are scheduled, the damage size distribution changes because defective parts are replaced with new parts having smaller damage sizes (fabrication defects, $a_{i,0}$). Reliability computation is very expensive when inspections are involved because crack size distribution has to be recharacterized after each inspection to simulate replacement, and exact computation of failure probability using MCS requires large sample size.

Harkness [1] developed an approximate method to expedite reliability computation with inspection by assuming that repaired components will never fail again, and he incorporated this assumption by modifying the FORM. The failure probability at any time following an inspection is the probability that the crack size is greater than the critical crack size at that time and that it has not been detected in any of the previous inspections. Using an empirical crack growth model like Eq. (3) to predict crack size at any time, a probabilistic model for inspection probability of detection, and a specified value of critical crack size, he calculated the structural reliability using FORM. The effect of inspections is incorporated into FORM by integrating the probability density function (PDF) of undetected cracks over the failure region using numerical integration. The assumption that detected cracks are replaced and the new component will not fail during the remainder of service life greatly simplifies the numerical computation by considering only the PDF of undetected cracks.

When inspections are needed earlier than half the service life, repaired components may have a large probability of failure and Harkness's method may not be accurate enough. Kale et al. [25] proposed an approximate method to simulate inspection and repair using MCS with small sample size to update the crack size mean and standard deviation after an inspection and FORM to calculate the failure probability between inspections. Estimating a low probability of failure using MCS is very expensive, for example, estimating P_f of 10^{-7} will require about 10^9 samples. The combined MCS and FORM approach can calculate failure probability with many fewer samples (50,000 used in this paper). The procedure described below expedites the reliability calculations by removing the need of MCS with large sample size.

A. Searching for Next Inspection Time Using FORM

The main computation associated with determining the inspection schedule for a given structure is to find the next inspection time at which the structural reliability will be lower than the specified threshold value. The probability of failure after N cycles of loading since the most recent inspection is defined as the event that fatigue life N_f is less than N.

$$P_f(N, a_i, m, \sigma) = P\lfloor N_f(a_i, m, \sigma) < N \rfloor \tag{12}$$

where a_i is the crack size distribution at the beginning of the inspection period and N_f is the number of cycles accumulated in growing a crack from a_i to a_c. For a given structural thickness, the next inspection time is obtained such that the probability of failure before the inspection is just equal to the maximum allowed value (Pf_{th}, reliability constraint). The next inspection time S_n for a given threshold reliability level is obtained by solving Eq. (13).

$$P\lfloor N_f(a_i, m, \sigma) - N \rfloor < Pf_{\text{th}} = 0 \tag{13}$$

Equation (13) is solved for time interval N by using a bisection method between the previous inspection time S_{n-1} and service life S_l and for each of the bisection iterations, the first term is calculated by FORM described in Sec. II.C. For an unstiffened panel FORM is very cheap; however, for a stiffened panel, while much cheaper than MCS, it is computationally expensive because the calculation of fatigue life is expensive and an additional computational burden is added because of the bisection search between previous inspection time S_{n-1} and service life S_l.

B. Updating Crack Size Distribution After Inspection

The algorithm for simulating crack growth and inspections is shown in Table 2. After obtaining the next inspection time, the crack size distribution has to be updated after that inspection. This updated crack size distribution serves as the initial crack size distribution for the following inspection interval. The damage distribution after an inspection can easily be updated by using MCS with a relatively small sample size and is computationally very cheap compared to calculating probabilities. The crack size a_N after N cycle of fatigue loading was obtained by solving Eq. (3). To obtain the crack size mean and standard deviation after an inspection, we produce 50,000 random numbers for each random variable in Eq. (3) (a_i, m, σ) and obtain the final crack size a_N. We then simulate the inspection by using Eq. (11) with another random number for probability of detection. If the crack is detected the panel is replaced by a new one with a random crack size picked from the distribution of

Table 2 Pseudocode for updating crack size distribution after inspection occurring after N cycles from previous inspection

1) Generate a panel by a random vector of uncertain variables (a_i, m, and σ).
2) Solve Eq. (3) for crack size a_N after N cycles of fatigue loading for the panel using Newton's method or bisection (if Newton's method does not converge). Use of response surface approximation to alleviate computational cost is explained in [25].
3) Compute the probability of detection of crack a_N from Eq. (11), $P_d(a_N)$.
4) Generate a random number from a uniform distribution with bounds (0, 1) P_d^{rand}.
5) If $P_d(a_N) \geq P_d^{\text{rand}}$ then simulate replacement of defective component by generating a random crack $a_{i,0}$ for a new panel and set $a_N = a_{i,0}$, else keep a_N.
6) Store a_N for fitting probability distribution to crack sizes after inspection and go back to (1).
7) Stop after 50,000 random panels have been simulated and fit distribution to crack sizes.

manufacturing defects $a_{i,0}$. After all cracks are analyzed for detection, the updated crack sizes are used to fit a distribution and to obtain its mean and standard deviation. This serves as the initial crack distribution for the next inspection. For the data used in this paper the fabrication crack distribution was lognormal, and the distribution after inspections was also found to be best approximated in least-squares fit by lognormal distribution out of 12 analytical distributions in ARENA© software [26] (Takus and Profozich [27]). If better accuracy is needed then a distribution with more parameters can be fitted to the data. So in general, the present approach can be used with the MCS used to fit a new distribution for the crack sizes after each inspection. The accuracy of this method in calculating failure probability compared to MCS with large sample size is discussed in Appendix B.

It would be possible to use the same MCS procedure as described in Table 2 to calculate the probabilities of failure needed for scheduling inspections. However, because the required probabilities of failure are of the order of 10^{-8}, this would require a prohibitively large MCS. So instead we use FORM as described in Sec. III.A to calculate failure probabilities and MCS to update crack size distribution after inspection, taking advantage of the characterization of the crack distribution as lognormal. The crack size probability distribution after the inspection was estimated by fitting probability distribution to the crack size samples obtained from MCS.

To illustrate this approach, we calculated the actual probability of failure for two inspection times for a 2.00 mm thick unstiffened panel using the proposed method. The first inspection time of 9288 flights was calculated from Sec. III.A with a lognormal initial crack size distribution with mean of 0.20 mm and coefficient of variation of 0.35. The crack size distribution after this inspection was updated by the procedure of Table 2 using a crack growth time N of 9288 flights. The updated crack distribution was found to be lognormal with mean = 0.30 mm and cov = 0.86. The next inspection time of 15,540 flights was obtained from Sec. III.A using the updated crack distribution.

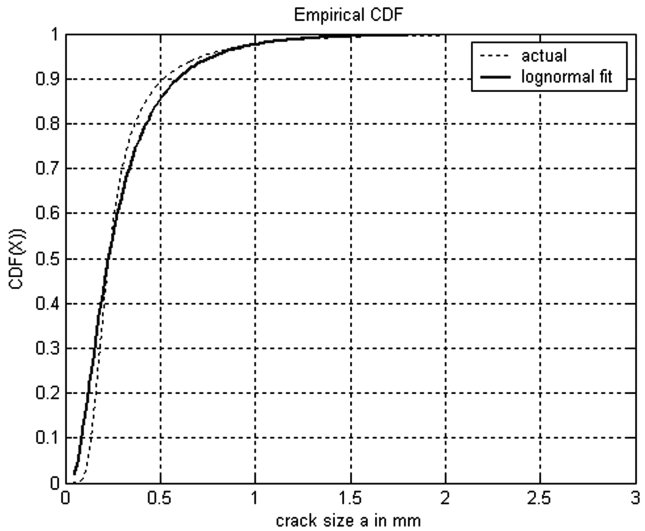

Fig. 2 Comparison of actual and lognormally fitted CDF of crack sizes after an inspection conducted at 9288 flights.

The goodness of fit of this distribution affects the accuracy of probability calculations. The actual and best fitted cumulative distribution functions (CDF) of crack size distribution after 9288 flights are shown in Fig. 2. The corresponding p value was less than 0.005 indicating a bad fit; however for low failure probabilities (e.g., 10^{-7}) this fit ensures accurate structural design calculation at very low computational expense. To validate this claim, the failure probability was calculated for the inspection schedule (first inspection = 9288, second inspection = 15, 540 flights) using MCS with 10^8 samples. The MCS failure probability after 9288 flights is 4.0×10^{-8} (lower than 10^{-7}) and after 15,540 flights is 2.7×10^{-7} (higher than 10^{-7}) which are close to the value of 10^{-7} calculated using the proposed method. The square error between the actual PDF and the lognormally fitted PDF is 0.00029 and the maximum error between CDFs is 0.06 at 0.28 mm.

C. Calculation of Inspection Schedule for a Given Structure

For a given structural design optimum inspections are added one by one until the probability at the end of service life is less than the specified threshold reliability level. Example 1 illustrates the approach described in Secs. III.A and III.B for a 2.0 mm thick unstiffened plate and a required reliability level of 10^{-7}. Using Sec. III.A to solve Eq. (13) for N, the first inspection time is 9288 flights. Crack growth simulation using the MCS pseudocode in Table 2 was performed with initial crack sizes $a_{i,0}$ and a crack growth time of 9288 flights giving the updated crack size distribution after the first inspection. The lognormal distribution fitted after inspection has a mean of 0.30 mm and coefficient of variation 86.0%. This serves as the initial crack size distribution for the second inspection. Again, the second inspection time was obtained as described in Sec. III.A as 15,540 flights. This cycle of scheduling inspections was continued until the failure probability at the end of service life was less than the specified value.

Figure 3 illustrates the variation of the probability of failure with and without inspection. Table 3 presents the inspection schedule during the service life and the crack size distribution parameters after each inspection. It can be seen that inspections are very helpful in maintaining the reliability of the structure. From Table 3 it can be seen that the first inspection interval is the largest. After the first inspection the repaired components are replaced with the same initial

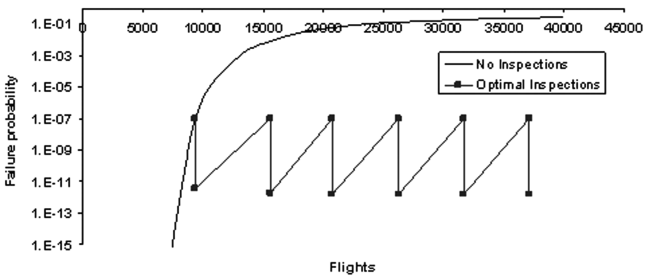

Fig. 3 Example 1, variation of failure probability with number of cycles for a 2.00 mm thick unstiffened panel with inspections scheduled for $Pf_{\text{th}} = 10^{-7}$.

Table 3 Example 1, inspection schedule and crack size distribution after inspection for an unstiffened plate thickness of 2.00 mm and a threshold probability of 10^{-7}

No. of inspections	Inspection time, S_n (flights)	Inspection interval (flights) $S_n - S_{n-1}$	Crack size distribution after inspection (mean, mm, cov)
0	——	——	Initial crack distribution (0.200, 35%)
1	9,288	9288	(0.300, 86%)
2	15,540	6252	(0.326, 90%)
3	20,741	5201	(0.335, 87%)
4	26,223	5482	(0.342, 87%)
5	31,649	5426	(0.345, 86%)
6	37,100	5451	(0.347, 86%)

Table 4 Cost factors, [28,29]

Density of aluminum, ρ	166 lb/ft^3
Fuel cost per pound per flight, F_c	\$0.015
Inspection cost, I_c	\$1 million
Material and manufacturing cost per lb, M_c	\$150.0
No. of panels, N_p	1350
Service life, S_l	40,000 flights

crack distribution (mean = 0.20 mm and cov = 35%); however, some cracks escape detection, leading to smaller inspection intervals. We can conclude that during the initial service life there is a fatigue induced aging because inspection intervals grow smaller. From the crack size distribution parameters shown in the last column of Table 3 we can conclude that the crack size distribution after each inspection essentially remains unchanged after a certain number of inspections, leading to uniform inspection intervals. We can infer that toward the end of service there is much less fatigue induced aging because the rate at which unsafe cracks are introduced in the structure due to replacement is the same as the rate at which cracks are detected by the inspections.

This paper assumes that when a defect is found the damaged part is replaced by a new part. As noted earlier, we can also incorporate a procedure that leaves very small cracks alone. To account for repair (instead of replacement) and repair induced damage would require information on the distribution of such damage. This is not addressed here.

D. Optimization of Structural Design

The cost associated with change in the structural weight for aluminum and the fuel cost was taken from [28]. He assumed a fuel cost of \$0.89 per gallon and that a pound of structural weight will cost 0.1 lb of fuel per flight. From this we calculated that a pound of structural weight will cost \$0.015 per flight for fuel. The structural weight is assumed to be directly proportional to the plate thickness and a pound of structural weight is assumed to cost \$150 for material and manufacturing. Kale [25] shows the details of material and fuel cost calculations. A typical inspection cost of about \$1 million was obtained from Backman [29]. Following [29] the service life is assumed to be 40,000 flights. The structural design parameters obtained for B747 series aircraft and cost factors are summarized in Table 4.

The life cycle cost C_{tot} for N_i inspections is

$$C_{\text{tot}} = M_c W + F_c W S_l + N_i I_c \tag{14}$$

where W is the total weight of all the panels in the fuselage, given as

$$W = N_p(N_s A_s b + thb)\rho \tag{15}$$

The parameters in Eqs. (14) and (15) are defined in the nomenclature.

Reliability-based design optimization is computationally very expensive when inspections are involved because several iterations on structural design variables and inspection times are required to find an optimum combination of structural sizes and inspections that will minimize total cost. For an unstiffened panel, analytical expression for crack growth is available and exact computations using the combined MCS and FORM technique are very cheap. For a stiffened panel, the crack growth has to be determined numerically and reliability computations are very expensive even with the combined MCS and FORM approach. Most of the computational expense goes to the calculation of the geometric factor due to stiffening, which can be determined using detailed finite element analysis or a displacement compatibility method due to Swift [5]. In this paper we used Swift's approach which takes about 0.5 s for evaluating a single value of a given structural design and crack length. Table 5 explains the various response surface approximations (RSAs) used to make computations faster. The computational time spent in construction of RSAs is shown in the last column of Table 5. Table 6 gives the breakdown of computational cost for calculation of exact inspection time and updating crack size distribution if the calculations were done without the use of RSA.

The last column in Table 6 show the errors made by the use of RSAs in calculations. An error of 0.02 is the typical fitting error in construction of RSA for ψ.

During the optimization the structural thickness t and the stiffener area A_s are changed, which changes the structural weight according to Eq. (15). The optimum inspection schedule is determined for this structural design using the procedure described in Table 7 and the total cost of structural weight and inspection is obtained from Eq. (14). The optimization iteration is stopped after a specified convergence tolerance is achieved. The convergence tolerance on minimum cost is assumed to be \$10,000 in this paper and the function

Table 5 Description of response surface approximations and computational time spent in their construction

Name of response surface	Description	Function of variables	Construction cost
ψ-RSA	Geometric factor due to stiffeners [25]	Skin thickness t_s, stiffener area A_s, crack length a	20 min
μ_{ai}-RSA	Crack size mean value after inspection [25]	Skin thickness t_s, stiffener area A_s, mean crack length μ_a, standard deviation in crack length σ_a, time N, standard deviation in stress σ_p	2 days
σ_{ai}-RSA	Crack size standard deviation after inspection [25]	Skin thickness t_s, stiffener area A_s, mean crack length μ_a, standard deviation in crack length σ_a, time N, standard deviation in stress σ_p	——
β_d-RSA	Reliability index [25]	Skin thickness t_s, stiffener area A_s, mean crack length μ_a, standard deviation in crack length σ_a, time N, standard deviation in stress σ_p	1 day

Table 6 Computational time that would be spent in exact calculation of next inspection time and updating of crack size distribution. Error due to ψ-RSA usage is given in last column

Variable	Computational method	No. of function evaluations	Total time, s	Typical error due to use of RSA
Geometric factor, ψ	Displacement compatibility	1	0.5	0.02 approximately
Fatigue life, N_f	Numerical integration using MATLAB's adaptive Simpson's quadrature	100 evaluations of ψ	50	600[a] flights (error in N_f due to error in ψ)
Reliability index, β_d	Iterative search using MATLAB's fmincon	100 evaluations of N_f	5000	0.2, average fitting error from β_d-RSA + 0.1[b] from error in N_f
Next inspection time, S_n	Bisection between S_{n-1} and service life S_l	15 evaluations of β_d	75,000 (0.86 days)	——
Crack size a_N after N cycles	Iterative search using Newton's method	20 evaluations of N_f	1000	——
Crack size distribution using Table 2	MCS	50,000 evaluations of a_N	50×10^6 (578 days)	Less that 0.1% from μ_{ai}-RSA and σ_{ai}-RSA. Pertinent error is on mean and standard deviation

[a]Assuming that the structure is designed for inspection intervals of 10,000 flights (typical results obtained in this paper), the error in fatigue life calculation due to error in ψ will be $10,000/(1.02)^m$, where m is the Paris law exponent. Using the mean value of $m = 2.97$ an error of 600 flights in fatigue life is obtained.
[b]The error in the reliability index consists of two parts: 1) the fitting error in the calculation of fatigue life due to RSA for N_f. For a typical inspection interval of 10,000 flights, an error of ± 600 flights in N_f due to RSA leads to an error of 0.1 in β_d; and 2) the average fitting error in RSA for β_d.

Table 7 Summary of computational method for combined optimization of structural design and inspection schedule

A) Optimization of structural design: For a given structural design optimize inspection schedule using step B and obtain cost of structural weight and inspections. Stop if convergence on minimum cost is obtained, otherwise update the structural design.

B) Optimization of inspection schedule: Add one inspection at a time using step C, update crack size distribution using step D. Check if the desired reliability level is satisfied at the end of service life using FORM, if not add one additional inspection.

C) Searching for next inspection time: Given structural sizes, probability distribution of random variables, find when the next inspection is needed by calculating the time S_n at which the probability of failure equals the required reliability level Pf_{th} using the first-order reliability method (FORM).
This is a computationally intensive optimization problem which requires repetitive computation of reliability index described in Sec. II.C. A rough estimate of computer time is given in Table 5.

D) Updating crack size distribution after inspection: After obtaining the next inspection time from Sec. III.B use Monte Carlo simulation (MCS) to update the crack size distribution after this inspection by growing cracks between the inspection time S_n and the previous inspection time S_{n-1}.
The MCS method is described in Sec. III.B and the computational expense associated with it is described in Table 6.
The computational burden associated with estimating crack size distribution parameters after an inspection is solved by using RSAs to estimate the crack size mean μ_{ai}-RSA and standard deviation σ_{ai}-RSA after an inspection. Kale [25] explains the details of these RSAs.

fmincon in MATLAB [22] is used to perform optimization of the design.

The main computational expense for the optimization is due to time spent in construction of RSAs. The ψ-RSA takes about 20 min, the μ_{ai}-RSA and σ_{ai}-RSA takes about 2 days and the β_d-RSA takes about 1 day. The calculations were performed on a Windows Pentium 4 machine. The use of RSAs to approximate the computationally expensive analyses (Table 6) made it feasible to solve this optimization problem.

Table 7 gives the overview of the methodology describing the computational challenge in its implementation and explains the approach used to perform reliability-based optimization of structural design and inspection schedule.

Table 8 Safe-life design of a stiffened panel

Required probability of failure, Pf_{th}	Minimum required skin thickness, t, mm	Life cycle cost $C_{\text{tot}} \times 10^6$	Structural weight, lb
10^{-7}	4.08	25.42	33,902
10^{-8}	4.20	26.16	34,880
10^{-9}	4.24	26.34	35,129

IV. Results

Structural design can have a large effect on operational cost and weight of the structure. When inspections and maintenance are not feasible, safety can be maintained by having conservative (thick) structural design. To demonstrate this we first obtain a safe-life design required to maintain a desired level of reliability throughout the service life for unstiffened and stiffened structures. Table 8 shows the safe-life design of an unstiffened panel and Table 9 shows the safe-life design of a stiffened panel.

An unstiffened panel is a single load path structure without load transfer capability. Comparing Tables 8 and 9, we see that if the structure is designed with a load transfer capability then the weight and cost can be reduced by about 10%. Stiffeners improve the load carrying capacity and reduce crack growth rates allowing greater crack length safely. This issue is further explored in [25].

Next we demonstrate the effect of inspections on structural safety and operational cost. Inspections improve the reliability by detecting and removing cracks. By optimizing the structural design together with the inspection schedule, we can trade structural weight against the inspection cost to reduce overall life cycle cost. To demonstrate the effectiveness of inspections, optimum structural designs and inspection schedules were first obtained for an unstiffened panel design with results shown in Table 10.

Table 9 Safe-life design of a stiffened panel

Required probability of failure, Pf_{th}	Total stiffener area 10^{-3} m^2, A_s	Skin thickness, t, mm	$\frac{A_s}{A_{\text{Total}}}100\%$	Life cycle cost, $C_{\text{tot}} \times 10^6$	Structural weight, lb
10^{-7}	2.23	2.31	35.85	22.42	29,900
10^{-8}	2.26	2.33	36.00	22.68	30,248
10^{-9}	2.30	2.35	36.22	22.91	30,555

Table 10 Optimum structural design and inspection schedule of an unstiffened panel (in all cases the optimum number of inspection is 3)

Required probability of failure, Pf_{th}	Skin thickness, t, mm	Optimum inspection times, S_n, flights	Life cycle cost, $C_{tot} \times 10^6$	Structural weight, lb
10^{-7}	2.30	12,346, 22,881, 31,365	17.28	19,109
10^{-8}	2.43	13,158, 23,496, 31,496	18.15	20,199
10^{-9}	2.56	13,927, 24,016, 31,682	18.97	21,295

Table 11 Optimum structural design and inspection schedule for stiffened panel

Required probability of failure, Pf_{th}	Total stiffener area, $A_s \times 10^{-4}$ m^2	Required skin hickness, t (mm)	$\frac{A_s}{A_{Total}}100\%$	Optimal inspection times, S_n, flights	Life cycle cost, $C_{tot} \times 10^6$	Structural weight, lb
10^{-7}	7.11	1.71	19.40	10,844, 18,625, 25,791, 32,908	17.20	17,659
10^{-8}	7.30	1.81	18.95	11,089, 18,758, 25,865, 32,943	17.87	18,504
10^{-9}	13.74	1.67	32.29	12,699, 22,289, 31,163	18.33	20,443

Table 12 Optimum structural design for regulations based inspections conducted at four constant interval or 8000 flights for stiffened panel

Required probability of failure, Pf_{th}	Total stiffener area $A_s \times 10^{-4}$ m^2	Required skin thickness, t, mm	$\frac{A_s}{A_{Total}}100\%$	Inspection times, S_n	Life cycle cost, $C_{tot} \times 10^6$	Structural weight, lb
10^{-7}	13.41	1.38	35.94	8,000, 16,000, 24,000, 32,000	17.44	17,927
10^{-8}	13.80	1.47	35.12	8,000, 16,000, 24,000, 32,000	18.16	18,878
10^{-9}	14.85	1.49	36.60	8,000, 16,000, 24,000, 32,000	18.61	19,491

By comparing Table 10 with Table 8, it can be seen that inspection and repair lower the life cycle cost by about 25% over the safe-life unstiffened panel design and by 20% over the stiffened panel safe-life design. The corresponding reductions in structural weight are 40% and 30%, respectively. There is an additional incentive for conducting inspections in that they protect against other types of damage like that due to accidental impacts and corrosion.

Next we optimize the structural design and inspection schedule for the stiffened panel design (Table 11) and illustrate the tradeoff of structural weight in skin and stiffeners against inspection cost.

Comparing Table 9 to Table 11 we see that inspections lower the life cycle cost of the stiffened panel design by about 20% compared to the safe-life design. Comparing Tables 10 and 11 we see only a small gain (about 3%) in designing stiffened structures when inspections are involved and cost can be minimized by designing single load path structures (unstiffened) with inspections. The increased design flexibility allows an additional tradeoff of structural weight against inspections by having one additional inspection over the unstiffened panel design. About 20 to 30% of the structural weight is transferred from skin to stiffeners.

In aircraft operation the inspection intervals are dictated by practical considerations and regulation which are based on service experience. The Joint Service Specification Regulations 2006 requires all airlines to conduct major depot level inspection 4 times during the service life. These inspections are conducted at uniform intervals. Table 12 shows the optimum design with a fixed inspection schedule.

It is seen that inspections done at constant intervals are only marginally less cost effective than the optimized inspection schedule. From Tables 10–12 we can conclude that when inspections are used to maintain safety there is less gain in using stiffeners for stable fatigue crack growth. However, stiffeners might be very useful in maintaining structural rigidity to resist buckling and pillowing. Also, from Table 9 when structures are designed without any inspections, stiffeners can be very helpful in reducing crack growth rate. Kale [25] discusses the effect of stiffening on structural design and crack growth rates.

Next we obtain optimum structural design and inspection times for a fixed number of inspections. Through this we seek to demonstrate the tradeoff of inspection cost against the cost of structural weight.

From Table 13 we see that the optimum structural weight decreases monotonically with the number of inspections because structural weight is traded against inspections. However, the stiffener areas show a sudden jump with the required number of inspections (decreasing inspections from four to three). The main reason for this is the presence of several local minima because the inspection cost is a discrete variable and any change in the number of inspections will lead to a large jump in either the skin thickness or the stiffener area if the total cost is minimized. In this case the stiffener areas show sudden change because stiffeners break during crack growth (reducing reliability) so that when the number of inspections is large, cost can be reduced by reducing stiffener areas and increasing structural thickness. The cost difference between these optima is very small. Actual failure probability was calculated for each of the local optima and the design whose failure probability was closest to the threshold value was selected. Exact evaluation of failure probability for some designs is discussed below. The ratio of stiffener area to skin area is constant at about 20% for when the number of inspections are large. For fewer inspections, about 30% of the structural weight is transferred to stiffeners. As more inspections are added the structural weight is traded against inspection cost until a minimum is reached; beyond this any further reduction in structural weight will lead to faster crack growth rate requiring frequent inspections to maintain reliability.

The optimum structural design and inspection schedule in Tables 8–13 were obtained by using RSAs with some approximation error. To determine actual reliability, we obtain reliability of the results in Table 11 using direct FORM. The β_d-RSA is not used to calculate the reliability index. Actual reliability is obtained by calculating the reliability index using FORM in Sec. II.C. The other RSAs described in Table 5 (ψ-RSA, μ_{ai}-RSA, σ_{ai}-RSA) are still used to reduce the computational time. Table 14 shows the actual reliability for the optimum structural design.

It can be seen that the error in the β_d-RSA results in errors of about a factor of 3 in the probability of failure. This error can be further reduced by using a more accurate (hence more costly) RSA. In addition to this error, the error from the RSA for ψ can affect the accuracy in the calculation of inspection time by 600 flights. Additional error is introduced because of convergence tolerance for calculation of reliability index (0.1 used in the paper) and randomness in MCS seed for calculating crack size distribution. The effect of RSA on accuracy of results and computational cost is explained in detail in Sec. III.D. Typically the optimum obtained from the RSA will be slightly different from the true optimum because of the error in the RSA. To get more accurate results, optima

Table 13 Tradeoff of inspection cost against cost of structural weight required to maintain fixed reliability level for stiffened panel

Required probability of failure, Pf_{th}	No. of inspection	Total stiffener area $A_s \times 10^{-4}$ m^2	Required skin thickness, mm	$\frac{A_s}{A_{\text{totsl}}}100\%$	Optimal inspection times, flights	Life cycle cost $\times 10^6$	Structural weight, lb
10^{-7}	5	7.05	1.60	20.26	9,497, 16,029, 22,064, 28,060, 34,036	17.53	16,714
10^{-7}	4	7.11	1.71	19.40	10,844, 18,625, 25,791, 32,908	17.20	17,659
10^{-7}	3	7.23	1.88	18.14[a]	12,743, 22,435, 31,212	17.35	19,140
10^{-8}	5	7.00	1.70	19.18	9,933, 16,406, 22,363, 28,271, 34,145	18.14	17,529
10^{-8}	4	7.30	1.81	18.95	11,089, 18,758, 25,865, 32,943	17.87	18,504
10^{-8}	3	13.29	1.63	32.04	12,514, 22,178, 31,110	18.03	19,945
10^{-9}	5	7.50	1.74	19.92	10,091, 16,428, 23,260, 29,268, 34,412	18.53	18,049
10^{-9}	4	7.89	1.88	19.51	11,546, 19,064, 26,064, 33,044	18.59	19,459
10^{-9}	3	13.74	1.67	32.29	12,699, 22,289, 31,163	18.33	20,443

[a]There exist another local minimum with $A_s = 14.64$ mm^2, $t_s = 1.505$ mm and inspection times of 12,375, 22,097, and 31,083 flights. However this design has slightly higher cost (2%), hence it is not shown in this table.

Table 14 Evaluation of structural reliability for optimum obtained from RSA for stiffened panel with inspection using direct FORM. The β_d-RSA is not used to calculate reliability index

Required reliability level, Pf_{th}	Optimum design (skin thickness mm, $\frac{A_s}{A_{\text{Total}}}100\%$)	Inspection times, flights	Actual Pf/Pf_{th} before each inspection
10^{-7}	1.71, 19.40	10,844, 18,625, 25,791, 32,908	2.89, 2.26, 1.98 , 3.90, 1.87
10^{-8}	1.81, 18.95	11,089, 18,758, 25,865, 32,943	0.98, 3.75, 3.35, 3.18, 3.06
10^{-9}	1.67, 32.29	12,699, 22,289, 31,163	2.12, 5.27, 1.47, 1.44

obtained from RSAs can be iteratively calibrated so that the actual failure probabilities are closer to the threshold value.

V. Conclusions

A computational method was developed using a combination of MCS and FORM to perform simultaneous optimization of structural design and inspection schedule. The method reduces computational cost in determining structural reliability with inspection. Response surface approximations were used to obtain crack growth to further reduce computational cost associated with reliability calculations. Optimum combinations of structural design and inspection schedule were obtained that will maintain the desired reliability level during service at a minimum cost. The paper also demonstrated the effectiveness of inspections for fatigue control and the tradeoff of structural weight against inspection cost for reliability For more complete failure models, inspections may be even more effective since they will also detect other damage modes besides cracks. Given additional computational resources, a more complete failure model can be easily included in the method developed in this paper. The important outcomes of this paper are as follows:

1) The combined MCS and FORM approach expedites reliability calculation with inspection compared to MCS with large sample size needed for accurate calculations. For the examples used in this paper, the combined MCS and FORM requires about 50,000 function evaluations compared to 10^9 or more for pure MCS.

2) Designing structures for multiple load transfer capability (that is stiffened panels) can be much more cost effective and failure resistant than single load path structures for a safe-life design; however, with inspections there is a much lower gain from stiffeners.

3) Inspections are most effective in maintaining reliability levels through damage detection and replacement.

For our examples, there was 25% in cost savings due to inspections over a safe-life design.

Appendix A: Calculation of Fatigue Life and Structural Cost

The calculation of fatigue life of a structural component is based on the equivalent initial flaw method [20]. According to this method all analytical calculations for crack growth are based on the assumption of a single initial flaw whose size is determined such that the fatigue life of a structure with this single initial defect is equal to fatigue life of a real structure with multiple defects. In this paper we assume that the aircraft fuselage is made of 1350 panels (all identical fatigue critical structural components) and each panel has one initial crack. Backman [29] and Tisseyre [30] 1994 determined inspection intervals for a specified reliability level for structurally significant items and assumed that aircraft is made of several of these items. Following them, the structural sizes and inspection time are determined so that the failure probability of a panel does not exceed the required reliability level specified for a panel. The fatigue critical cost of the entire aircraft is determined by calculation of the material and fuel cost of all 1350 panels. The total failure probability of aircraft will be more than that of a panel and can be calculated using system reliability; however, the reliability threshold is specified on a panel and not the entire aircraft and RBDO is performed for a panel.

Safe-life design: Structures designed for a fixed service life during which the probability of failure is very low. Inspections and replacement are not conducted.

Fail-safe design: Structural integrity is maintained by designing them for damage containment, crack arrest, and multiple load paths that preserve the limit load capability. Inspections are conducted at fixed intervals to repair damaged parts

Appendix B: Comparison of Present Method to Harkness Method

This Appendix compares the method of reliability calculation for the inspection schedule developed by Harkness [1] with the methodology proposed in this paper. The moment based method developed by Harkness simplifies the probability calculation by assuming that repaired components will not fail. This assumption can be easily incorporated in FORM to calculate failure probability and provides accurate results if inspections are scheduled after 50% of service life [1]. When inspections occur before 50% of service life, the FORM method of the repaired components may have a large probability of failure before the end of service. Here, Harkness's method will underestimate failure probability.

Table B1 Inspection schedule ($a_h = 0.63$ mm) for a 2.0-mm thick plate and a threshold probability of 10^{-6} developed using the Harkness method

No. of inspections	Inspection time (flights)	Failure probability calculated by Harkness method	Actual failure calculated by MCS
0	——	——	——
1	9,908	10^{-6}	6.20×10^{-7}
2	22,830	10^{-6}	9.83×10^{-4}
End of service	40,000	1.0×10^{-7}	2.15×10^{-2}

Table B2 Inspection schedule ($a_h = 0.63$ mm) for a 2.0-mm thick plate and a threshold probability of 10^{-4} developed using the Harkness method

No. of inspections	Inspection time (flights)	Failure probability calculated by Harkness method	Actual failure calculated by MCS
0	——	——	——
1	11,664	10^{-4}	7.14×10^{-5}
2	29,668	10^{-4}	2.95×10^{-2}
End of service	40,000	5.4×10^{-8}	1.04×10^{-4}

Table B3 Inspection schedule and crack size distribution after inspection ($a_h = 0.63$ mm) for a 2.0 mm thick plate and a threshold probability of 10^{-6} developed using the proposed method

No. of inspections	Inspection time (flights)	Failure probability calculated by proposed method	Actual failure calculated by MCS	Crack size distribution after inspection (mean, mm, cov)
0	——	——	——	Initial crack distribution (0.200, 0.35)
1	9,908	10^{-6}	5.60×10^{-7}	(0.272, 1.04)
2	16,298	10^{-6}	4.61×10^{-6}	(0.260, 1.05)
3	22,914	10^{-6}	9.00×10^{-7}	(0.255, 1.06)
4	29,470	10^{-6}	1.16×10^{-6}	(0.252, 1.07)
5	36,020	10^{-6}	1.06×10^{-6}	(0.250, 1.07)
End of service	40,000	9×10^{-8}	$<1.00 \times 10^{-8}$	——

Table B4 Inspection schedule and crack size distribution after inspection ($a_h = 0.63$ mm) for a 2.0 mm thick plate and a threshold probability of 10^{-5} developed using the proposed method

No. of inspections	Inspection time (flights)	Failure probability calculated by proposed method	Actual failure calculated by MCS	Crack size distribution after inspection (mean, mm, cov)
0	——	——	——	Initial crack distribution (0.200, 0.35)
1	11,664	10^{-4}	7.00×10^{-5}	(0.272, 1.09)
2	22,709	10^{-4}	1.54×10^{-4}	(0.260, 1.30)
3	32,653	10^{-4}	8.36×10^{-5}	(0.244, 1.28)
End of service	40,000	1.10×10^{-5}	1.17×10^{-5}	——

To compare the two approaches we calculate the inspection schedule using 1) the Harkness method and 2) the method proposed in this paper, and calculate the failure probability at the inspection times using MCS with 5×10^7 samples. First we calculate the inspection times for a 2.0 mm thick unstiffened plate, necessary to maintain threshold reliability levels of 10^{-6} and 10^{-4} using the method developed by Harkness (repaired cracks never fail) and calculate the probability of failure at these inspection times using MCS with 5×10^7 samples. The reliability level of 10^{-6} is chosen because it is close to a reasonable target reliability, but for that level MCS has substantial errors. The reliability level of 10^{-4} allows us to obtain MCS results that are accurate to about 2%.

Tables B1 and B2 show that at the first inspection the Harkness method is reasonably accurate, with the error coming from the FORM approximation. However, after repair (second inspection) the actual failure probability calculated by large MCS simulation (5×10^7 samples) is much higher than that calculated by the Harkness method. Tables B3 and B4 show similar calculations for the method proposed in the present paper. The difference between the MCS values in the tables for the first inspections gives us a measure of the scatter in the MCS calculations. After the first inspections the tables diverge, with the results of the proposed method being much more accurate. We can see that the pure MCS results are approximated well by the combined MCS-FORM approach proposed in this paper.

Appendix C: Effect of Threshold Crack Size for Detection

It is assumed that once a crack is detected, the panel is replaced by a newly manufactured panel with the fabrication defect distribution. This is not reasonable when we can detect very small cracks, and the present procedure allows us to consider a scenario where only cracks above a certain size trigger replacement of the panel. We calculate probability of failure after an inspection using 10×10^6 samples. When a crack is detected in an inspection, replacement is made only if the crack size is greater than a specified threshold for replacement. The results are presented in Table C1.

Table C1 shows the failure probability calculated with MCS of size 10×10^6. The second column shows failure probability computed using the assumption that when a crack is detected it is repaired (this cracks is replaced by a new one with the initial crack

Table C1 Probability of failure after inspection ($a_h = 0.63$ mm) for a 2.0 mm thick plate and a threshold probability of 10^{-5}

Inspection time (flights)	Actual failure calculated by MCS (all detected cracks are repaired)	Failure probability calculated by MCS (threshold crack size for replacement = 4.5 mm)	Failure probability calculated by MCS (threshold crack size for replacement = 1.5 mm)	Failure probability calculated by MCS (threshold crack size for replacement = 0.9 mm)
11,664	7.00×10^{-5}	7.15×10^{-5}	7.73×10^{-5}	7.80×10^{-5}
22,709	1.54×10^{-4}	5.12×10^{-3}	1.56×10^{-4}	1.56×10^{-4}
32,653	8.36×10^{-5}	1.13×10^{-3}	1.35×10^{-4}	9.09×10^{-5}
40,000	1.17×10^{-5}	3.69×10^{-5}	1.72×10^{-5}	1.26×10^{-5}

distribution $a_{i,0}$). The third column shows the pf when all the detected cracks below a threshold value of 4.5 mm are not repaired, etc. The results show that no significant difference in failure probability calculation is introduced by assuming that cracks below 1.5 mm are skipped repair compared to our assumption that all cracks are repaired.

Appendix D: Stress Intensity Factor of Stiffened Panel

As the crack propagates in a stiffened panel, the load is transferred from the skin to the intact stiffeners by means of fasteners. The stress intensity factor at the crack tip can be obtained by displacement compatibility analysis. In this method the displacement in the cracked sheet at the fastener location is made equal to the stiffener plus fastener displacement. The effect of stiffening is measured by the geometric factor which is the ratio of the stress intensity factor with stiffening to that without stiffening.

To demonstrate the application of the displacement compatibility analysis we consider a center cracked stiffened panel with two intact stiffeners placed symmetrically across from the crack centerline and a broken stiffener along the crack centerline. This is a typical example of a two bay cracks with a center broken stiffener used to certify aircraft for damage tolerance.

The stress intensity factor at the crack tip of a stiffened panel is lower than that on an unstiffened panel because of the reduced stresses at the crack tip. The panel is assumed to be in a state of plane stress and the stiffeners are assumed to be one-dimensional rods placed symmetrically across the crack with one broken stiffener along the crack centerline. The displacements in the panel at fastener locations are obtained by superposition of five cases as follows:

1) V1, the displacement anywhere in the cracked sheet caused by the applied gross stress,

2) V2, the displacement in the uncracked sheet resulting from fastener loads,

3) V3, the displacement in the uncracked sheet resulting from broken fastener loads,

4) V4, the displacement in the cracked sheet resulting from stress applied to the crack face equal and opposite to the stresses caused by rivet loads,

5) stiffener displacement resulting from direct fastener load.

For displacement compatibility the stiffener plus fastener displacement at any location should be equal to skin displacement at that location. These equations can be solved for fastener forces and the stress intensity factor can be determined using the resulting stress at crack tip.

Acknowledgments

This research is supported by the NASA Constellation University Institute Project, CUIP (formerly the University Research Engineering and Technology Institutes, URETI) Grant NCC3-994 of the Institute for Future Space Transport (IFST) at the University of Florida and NASA Grant NAG1-02042. The authors thank Thomas Swift for providing valuable input in implementing the displacement compatibility method for calculating the effect of stiffening on stress intensity.

References

[1] Harkness, H. H., "Computational Methods for Fracture Mechanics and Probabilistic Fatigue," Ph.D. Dissertation, Department of Mechanical Engineering, Northwestern University, Evanston, IL, 1994.

[2] Harkness, H. H., Fleming, M., Moran, B., and Belytschko, T., "Fatigue Reliability Method with In-Service Inspections," *FAA/NASA International Symposium on Advanced Structural Integrity Methods for Airframe Durability and Damage Tolerance, NASA Conference, Part I*, Langely Research Center, Hampton, 1994, pp. 307–325.

[3] Kale, A. A., Haftka, R. T., Papila, M., and Sankar, B. V., "Tradeoff for Weight and Inspection Cost for Fail-Safe Design," AIAA Paper 2003-1501, 2003.

[4] Kale, A. A., Haftka, R. T., and Sankar, B. V., "Tradeoff of Structural Weight and Inspection Cost in Reliability Based Optimum Design Using Multiple Inspection Types," AIAA Paper 2004-4404, 2004.

[5] Swift, T., "Fracture Analysis of Stiffened Structure," American Society for Testing of Materials, Special Technical Publication, ASTM STP 842, 1984, pp. 69–107.

[6] Yu, J. C., "Stress Intensity Factor for an Edge Crack in a Stiffened Sheet," American Society for Testing of Materials, ASTM STP 945, 1988, pp. 247–258.

[7] Nees, C. D., and Canfield, R. A., "Methodology for Implementing Fracture Mechanics in Global Structural Design of Aircraft," *Journal of Aircraft*, Vol. 35, No. 1, 1998, pp. 131–138.

[8] Arietta, A. J., and Striz, A. G., "Modelling of Aircraft Fatigue Load Environment," AIAA Paper 00-0973, 2000.

[9] Arietta, A. J., and Striz, A. G., "Optimal Design of Aircraft Structures with Damage Tolerance Requirements," *Structural and Multidisciplinary Optimization*, Vol. 30, No. 2, 2005, pp. 155–1631.

[10] Provan, J. W., and Farhangdoost, K., "A New Stochastic Systems Approach to Structural Integrity," *FAA/NASA International Symposium on Advanced Structural Integrity Methods for Airframe Durability and Damage Tolerance, NASA Conference, Part I*, Langely Research Center, Hampton, 1994, pp. 603–619.

[11] Brot, A., "Probabilistic Inspection Strategies for Minimizing Service Failures," *FAA/NASA International Symposium on Advanced Structural Integrity Methods for Airframe Durability and Damage Tolerance, NASA Conference, Part I*, Langely Research Center, Hampton, 1994, pp. 99–109.

[12] Fujimoto, Y., Kim, S. C., Hamada, K., and Huang, F., "Inspection Planning Using Genetic Algorithm for Fatigue Deteriorating Structures," *Proceedings of the International Offshore and Polar Engineering Conference*, Vol. 4, International Society of Offshore and Polar Engineers, Golden, 1998, pp. 461–468.

[13] Toyoda-Makino, M., "Cost-Based Optimal History Dependent Strategy for Random Fatigue Cracks Growth," *Probabilistic Engineering Mechanics*, Vol. 14, No. 4, Oct. 1999, pp. 339–347.

[14] Enright, M. P., and Frangopol, D. M., "Reliability Based Lifetime Maintenance of Aging Highway Bridges," *Proceedings of SPIE 5th International Symposium on Nondestructive Evaluation and Health Monitoring of Aging Infrastructure*, SPIE, Bellingham, WA, 2000, pp. 4–13.

[15] Wu, J. Y., Millwater, R. Y., Enright, M. P., Chell, G. G., Kuhlman, C. J., and Leverant, G. R., "Probabilistic Method for Design Assessment of Reliability with Inspection (DARWIN)," AIAA Paper 00-1371, 2000.

[16] Garbatov, Y., and Soares, C. G., "Cost and Reliability Based Strategies for Fatigue Maintenance Planning of Floating Structures," *Reliability Engineering and Systems Safety*, Vol. 73, No. 3, 2001, pp. 293–301.

[17] Wu, J., and Shin, Y., "Probabilistic Damage Tolerance Methodology for Reliability Design and Inspection Optimization," AIAA Paper 04-1789, 2003.

[18] Wu, J., and Shin, Y., "Probabilistic Function Evaluation System (ProFES) for Maintenance Optimization," AIAA Paper 2005-2214, 2005.

[19] Niu, M. C., *Airframe Structural Design, In: Fatigue, Damage Tolerance and Fail-Safe Design*, Conmilit Press Ltd., Hong Kong, 1990, pp. 538–570.

[20] JSSG-2006, "Joint Service Specification Guide," Department of Defense, 1998.

[21] Jackson, P., *Jane's All The World's Aircraft*, ISBN 0 710612621, International Thomson Publishing Co., London, 1995–1996.

[22] MATLAB Ver. 6.5.0, Copyright Mathworks, Inc., Natick, MA, 1984–2002.
[23] Palmberg, B., Blom, A. F., and Eggwertz, S., "Probabilistic Damage Tolerance Analysis of Aircraft Structures," *Probabilistic Fracture Mechanics and Reliability*, Martinus–Nijhoff, Dordrecht, The Netherlands, Vol. 10, 1987, pp. 47–130, A87-3528615-38.
[24] Rummel, W. D., and Matzkanin, G. A., *Non Destructive Evaluation Capability Data Book*, 3rd ed., Nondestructive Testing Information Analysis Center, Austin, 1997.
[25] Kale, A. A., Haftka, R. T., and Sankar, B. V., "Reliability Based Design and Inspections of Stiffened Panels," AIAA Paper 2005-2145, 2005.
[26] ARENA Ver. 3.01., Copyright 1997, System Modeling Corporation, Milwaukee, WI.
[27] Takus, D. A., and Profozich, D. M., "Arena Software Tutorial," *Proceedings of the Winter Simulation Conference*, Institute for Operations Research and the Management Sciences, Atlanta, 1997.
[28] Venter, G., "Non-Dimensional Response Surfaces for Structural Optimization with Uncertainty," Ph.D. Dissertation, Department of Mechanical and Aerospace Engineering, Univ. of Florida, Gainesville, FL, 1998.
[29] Backman, B., "Structural Design Performed to Explicit Safety Criteria Containing Uncertainties," AIAA Paper 01-1241, 2001.
[30] Tisseyre, M., Plantec, J. Y., Beaufils, J. Y., and Boetsch, R., "Aerospatiale Probabilistic Methods Applied to Aircraft Maintenance," Aerospatiale, Toulouse, France, 1991.